Solar Energy 177 (2019) 440–447

Contents lists available at ScienceDirect

Solar Energy

journal homepage: www.elsevier.com/locate/solener

Continuous oscillation of a compact solar-pumped Cr, Nd-doped YAG ceramic rod laser for more than 6.5 h tracking the sun

Yasuhiro Suzuki[a], Hiroshi Ito[a], Takaya Kato[b], Luu Thi An Phuc[c], Kemmei Watanabe[b], Hidetaka Terazawa[b], Kazuo Hasegawa[d], Tadashi Ichikawa[d], Shintaro Mizuno[d], Akihisa Ichiki[a], Satoshi Takimoto[b], Akio Ikesue[a], Yasuhiko Takeda[d], Tomoyoshi Motohiro[a,b,d,*]

[a] Green Mobility Research Institute, Institute for Innovation for Future Society, Nagoya University, Chikusa-ku, Nagoya 464-8603, Japan
[b] Graduate School of Engineering, Nagoya University, Chikusa-ku, Nagoya 464-8603, Japan
[c] School of Transportation Engineering, Hanoi University of Science and Technology, No 1 Dai Co Viet, Hai Ba Trung, Hanoi, Viet Nam
[d] Toyota Central Research and Development Laboratories, Inc., Nagakute, Aichi 480-1192, Japan

ARTICLE INFO

Keywords:
Continuous oscillation
Solar-pumped laser
Cr, Nd-doped YAG ceramic
Natural/air convection

ABSTRACT

Remaining key challenges for solar-pumped lasers (SPLs) to be applied for terrestrial solar energy utilization are (1) improvement of energy conversion efficiency and (2) ability of continuous laser oscillation during the day time. To address the latter challenge (2), a compact SPL employing a rigid 76.2 mm caliber paraboloidal mirror and a 10 mm-long, 1 mm diameter Cr, Nd-doped YAG ceramic rod was developed to realize more stable oscillation performance by introducing rapid cooling by free/natural air convection and increased mechanical stability during wind exposure in contrast to the conventional large solar pumped lasers (SPLs) employing typically a 2 m size conversing lens or mirror. Arrays of the compact SPLs could be used for harvesting sunlight across a large area. Outdoor, solar tracking experimentation with the compact SPL yielded continuous oscillation exceeding 6.5 h, improving upon previously determined maximum continuous oscillation times of 11 min. This is an indispensable experimental step if SPLs are to be applied to terrestrial solar energy utilization.

1. Introduction

Solar-pumped (or sun-pumped) lasers (SPLs) can be used as a non-contact method to transmit collected solar energy across large distances. Some examples include power transmission between an orbiting or lunar power station and the ground (Mori et al., 2004), between deep-sea and sea-level, or for powering mobile objects such as drones, robots, or electric vehicles (Motohiro et al., 2017). Additionally, SPLs have been investigated in photo-thermal and photo-chemical applications to promote MgO reduction in the Mg energy cycle by a research group of Tokyo Institute of Technology (TIT) (Ohkubo et al., 2009) and have been proposed for an application to dissociation of deep-sea methane hydrate by transmission of renewable SPL laser power via optical fibers (Ide, 2017). In spite of these various future potential applications, SPLs have come up against two blank walls: (1) low sunlight-to-laser energy conversion efficiency and (2) short continuous oscillation. The present work addresses the second blank wall (2) and was successful attaining continuous oscillation for more than 6 h and 30 min. This is an indispensable step for SPLs to be used in the practical solar energy utilizations. We are also addressing the blank wall (1) and it is briefly mentioned in the discussion section although its detail has been and is to be reported elsewhere.

SPLs were reported in 1960s (Kiss et al., 1963; Simpson, 1964; Young, 1966), soon after the discovery of laser, i.e., stimulated optical radiation in ruby (Maiman, 1960). Those initial works of SPLs employed mainly laser mediums (LMs) of Nd-doped yttrium aluminum garnet (Nd:YAG) single crystals. Since then, 570 papers which are electronically accessible or more have been published on SPLs. Iodine or iodides used to be major laser LMs intensively studied by groups of USA (NASA, University of Florida, etc.) (Lee and Weaver, 1981; Terry et al., 1996), and Russia (Institute of Laser Physics, etc.) (Belousova et al., 2001). Then, transparent Nd:YAG ceramic laser rods were successfully fabricated and used as one of major LMs (Ikesue and Aung, 2008; Ikesue et al., 2013). Further, Cr and Nd-doped YAG (Nd/Cr:YAG) ceramics have been intensively studied by Institute for Laser Technology, Osaka and Institute of Laser Engineering, Osaka University,

Abbreviations: SPL, solar-pumped laser; YAG, yttrium aluminum garnet; OAP, off-axis parabolic mirror; NA, numerical aperture; BPF, band pass filter; BBAR, broadband antireflection coating; OC, output coupler

* Corresponding author.
E-mail address: motohiro@gvm.nagoya-u.ac.jp (T. Motohiro).

https://doi.org/10.1016/j.solener.2018.10.071
Received 18 February 2018; Received in revised form 23 October 2018; Accepted 25 October 2018
Available online 23 November 2018
0038-092X/

Japan (Saiki et al., 2008). Some of these studies have been performed under collaborations with Japan Aerospace Exploration Agency (JAXA) in connection with applications of SPLs to space solar power systems (Mori et al., 2004). Applications of SPLs to thermal reduction of MgO in the "MgO energy cycle" has been proposed and intensively studied by a research group of Tokyo Institute of Technology (TIT), Japan (Ohkubo et al., 2009). Nd-doped ZrF_4–BaF_2–LaF_3–AlF_3–NaF glasses have been studied for LMs for solar pumped fiber lasers by Toyota Institute of Technology, Japan (Suzuki et al., 2011). More recently, transverse excitation was introduced into a solar pumped fiber laser system to decrease the threshold excitation power for oscillation using a low sunlight concentration at the ratio of 1/15 by Tokai University and Toyota Motor Corporation, Japan (Masuda et al., 2017). A thin-disk-shaped medium for SPL has been also proposed by the same group (Endo, 2007) [14]. Ongoing SPL research has been performed by Academy of Sciences of Uzbekistan (Payziyev and Makhmudov, 2016). Weizmann Institute of Science, Israel (Pe'er et al., 2001), and the research group of NOVA university of Lisbon, Portugal (Almeida et al., 2015; Liang et al., 2017) have been making great contributions to the research of SPLs.

In one of the early papers (Young, 1966), a water-cooled Nd:YAG crystal rod was pumped with a 61-cm diam., solar tracking, equatorial mount solar collector to give 1 W of continuous wave (CW) laser output. Although we can find the following description: "Operation over many hours was obtained with no evidence of reduction of output.", no evidential data of continuous oscillation was given in this paper. An evidential record of continuous oscillation for 11 min was reported employing a water-cooled Nd:YAG rod and a 10 m aperture solar collector (Arashi et al., 1984), in which tracking error was corrected manually 8–10 times during this 11 min continuous operation. A record of 60 sec stable continuous oscillation was also reported employing a water-cooled Nd:YAG ceramic rod and 2 m × 2 m Fresnel lens to generate 110 W CW laser output by TIT (Dinh et al., 2014). Pulsed emissions of laser for 30 min from a solar pumped Nd:YAG ceramic triggered by a Nd:YAG high-repetition pulsed laser was also reported (Saiki et al., 2017). In this case, since the solar-pumped Nd:YAG ceramic was used as an active-mirror amplifier of a seed Nd:YAG high-repetition pulsed laser, we exclude this from the reported data of genuine continuous oscillation experiments mentioned above. More recently, records of continuous oscillation of solar-pumped 1064 nm laser emission with a simple Gaussian intensity distribution around the center axis of the beam (TEM_{00}-mode) for 4 min were reported by the research group of NOVA university of Lisbon (Mehellou et al., 2017).

In these previous studies, Fresnel lenses or Cassegrain type conversing mirrors of typically 2 m in diameter were used to harvest sunlight. However, the large system accompanied by a large equatorial mount is apt to be mechanically unstable against wind. The focused sunlight in the large LM such as a Nd:YAG crystal or a ceramic of typically 10 mm in diameter and 100 mm in length causes temperature inhomogeneity because of poor thermal dissipation even if water-cooling is employed. The temperature inhomogeneity causes inhomogeneity of refractive index in the medium and brings the optical power density distribution out of the laser oscillation mode. Therefore, oscillation becomes unstable and apt to cease frequently, as has been observed in prior experiments, yielding a record continuous oscillation of 11 min tracking the sun. Since we have been proposing development of SPLs as the devices for terrestrial solar energy utilization (Motohiro et al., 2017), continuous oscillation during daytime is critical. To attain stable continuous oscillation of SPL during the daytime, we made SPL compact down to 50 mm in aperture diameter of the mirror (Ito et al., 2012; Mizuno et al., 2012), so as to be more robust to wind load and more prone to stable continuous oscillation due to its smaller stature and effective heat dissipation by free/natural air convection, respectively. Hereafter, our SPL is expressed as μSPL in this paper. The drawback of this downsizing is the decrease in available ground area for sunlight harvesting. To cope with this drawback and compensate the small aperture area of a single SPL for sunlight harvesting, a coordinated solar tracking system of an array of μSPLs were proposed and fabricated for outdoor test (Motohiro et al., 2015) as schematically shown in Fig. 1.

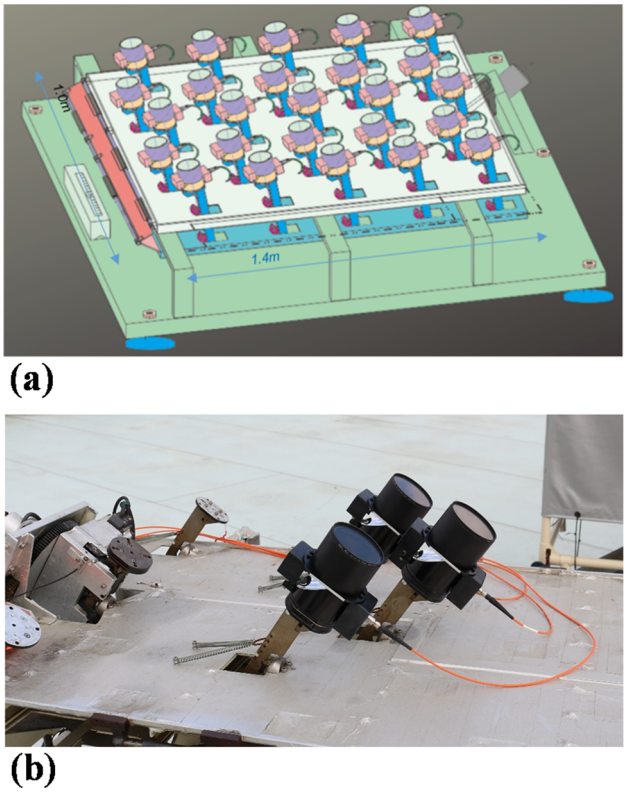

Fig. 1. Schematic of an array of 25 SPLs on a coordinated solar tracking system (a), and a photograph of an outdoor test of the coordinated solar tracking system on which SPLs are installed on 3 of 25 mounts (b).

We have been trying to extend the time of continuous oscillation from 10 min (Mizuno et al., 2014) to 1 h (Motohiro et al., 2017). Here, we present detailed experimental data of continuous oscillation of our specially designed μSPL for more than 6 h 30 min from 10:50 to 17:33, tracking the sun automatically.

2. Experimental

Before the detailed descriptions of our μSPL, our basic strategy to attain a longer continuous oscillation is presented. To achieve longer continuous oscillation operation, temperature rise across the LM must be reduced through increased thermal dissipation from the surface of LM. Fig. 2 displays variation of surface area under the constant cylindrical volume of the LM as a function of the aspect ratio defined by length/diameter of a cylindrical LM. Both disk-type and fiber LMs have larger surface area to volume ratios than rod-type LMs, resulting in increased thermal dissipation by free/natural convection. As for disk-type LMs, employment of a vertical cavity surface emitting laser (Quarterman and Wilcox, 2015) is to be discussed as a future choice in the Discussion section in this paper. As for fiber LMs, we had already attained laser oscillation under the sunlight using the μSPL apparatus similar to the present study previously (Mizuno et al., 2012). In this case, however, we had not been successful in doping Cr in Nd-doped ZrF_4–BaF_2–LaF_3–AlF_3–NaF glass fibers (Suzuki et al., 2011). This caused a reduced spectral matching efficiency for the sunlight as low as 15%, almost one half of Nd/Cr:YAG ceramic rod medium, while the mode matching efficiency in the fiber medium was as large as 80%, in comparison to 29% of the present Nd/Cr:YAG ceramic rod medium. Since we estimated that we could attain the same laser output with that of the fiber medium, we divided the fiber into many short pieces to make an

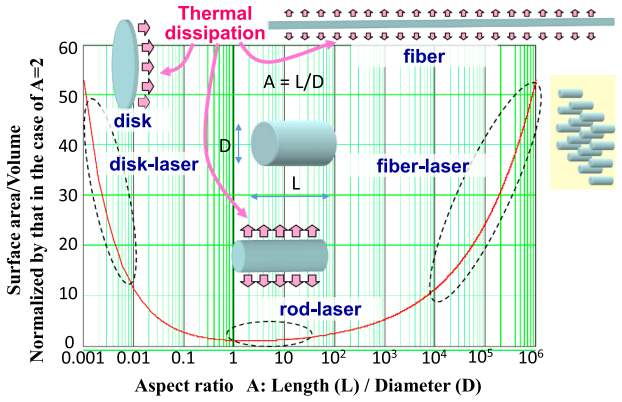

Fig. 2. Variation of surface area under the constant cylindrical volume of the LM as a function of the aspect ratio (A) defined by length (L)/diameter (D). The improvement of the surface area, that is, the improvement of thermal dissipation from the conventional thick rod type LM shown in lower center indicated in upper left is attained by a disk-shaped LM as shown by an inserted graphic. The improvement in upper right is attained by a fiber LM as shown in the inserted graphic. The same thermal dissipation and laser output power can be attained by an array of micro rods, that is, the divided fiber mediums with the same sunlight input as indicated in the right side. This is the base of our strategy on μSPL.

array, that is, an array of micro rods with the same diameter as the fiber and with the same concentrator for each rod medium as displayed in the graphic inserted at the right side in Fig. 2, and we made the array receive the same total amount of the sunlight. In the case of the array of micro rods, we can use Nd/Cr:YAG ceramics which has almost twice as high spectral matching efficiency as the Nd-doped ZrF_4–BaF_2–LaF_3–AlF_3–NaF glass fibers. This is our basic strategy to employ an array of micro Nd/Cr:YAG ceramic rods with converging mirrors much smaller than in the conventional SPLs.

Fig. 3 illustrates the core components of our SPL, and Captions for the abbreviations in Fig. 3 are summarized in Table 1. In our SPL, a 76.2 mm caliber off-axis parabolic mirror (OAP, Edmund Optics, #63-187) of aluminum covered with an aluminum coating layer of reflectance R ≒ 95% was employed for concentration of sunlight at the ratio of 1×10^{-4}. A UV filter (Kenko Tokina Zeta UV L41) was attached at the entrance of the OAP caliber in order to prevent

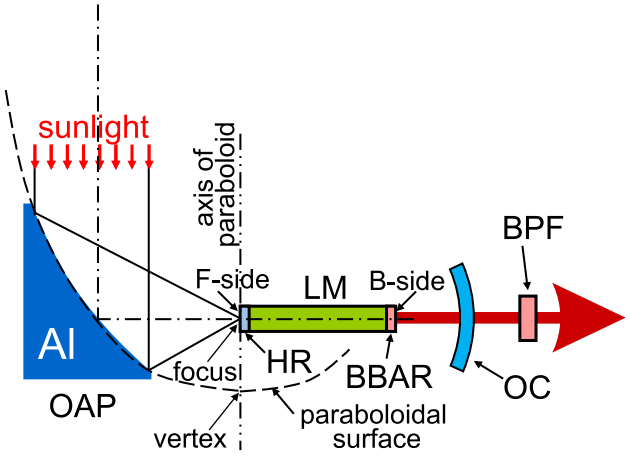

Fig. 3. Schematic illustration of the core components of μSPL developed in this work. OAP, LM, HR, BBAR, OC, BPF stand for Off-axis paraboloidal mirror, LM, High reflection coating on F-side of LM, Broadband antireflection coating on B-side of LM, Output coupler, and Band pass filter, respectively (cf. Table 1). The paraboloidal surface extended from the reflecting surface of OAP is indicated with a broken line as well as the axis of paraboloid in a dashed-two dotted line, the focus and the vertex of paraboloid.

colorization (solarization) of LM. In previous studies, much larger concentrators with lower concentration ratios around 4×10^{-4} such as 2 m × 2 m Fresnel lens or Cassegrain-type concave mirrors of a 2 m caliber have been used (Young, 1966; Lee and Weaver, 1981; Terry et al., 1996; Belousova et al., 2001; Payziyev and Makhmudov, 2016; Pe'er et al., 2001; Liang et al., 2017; Arashi et al., 1984; Dinh et al., 2014).

The diameter of the caliber of the OAP was 1.5 times larger than our μSPL of a 50.8 mm caliber in our previous report (Ito et al., 2012; Mizuno et al., 2012, 2014; Motohiro et al., 2015, 2017). The high sunlight concentration ratio of 1×10^{-4} requires adjustment of direction of incident sunlight within 1 mrad. The μSPL included a cylindrical LM made of transparent YAG ceramic cylindrical rod doped with 1% Nd and 0.1% Cr of 1 mm in diameter and 10 mm long without forced air or water-cooling as has been required in larger, conventional SPLs. The concentrated sunlight was focused on the F-side edge of LM. Since we used OAP, the geometry of optical concentration was asymmetric around the center axis of LM, and the maximum incident angle of the focused sunlight against F-edge surface of LM varied between 30° and 44.4° depending on the reflection point on the mirror. The focal image of the sun around 0.5 mm in diameter is smaller than the diameter of the F-side edge of LM. This edge of LM were optically polished and coated with a thin film optical filter (HR). The B-side edge of LM was also optically polished and coated with a thin film optical filter (BBAR). OC was located on the output pass of the laser to compose the resonator. BPF was also located on the output pass of the laser to transmit the laser light selectively. In place of the altazimuth used in our previous study (Motohiro et al., 2017), the μSPL was mounted on a VIXEN SXD2 equatorial mounting with a tripod stand which is commercially available from Vixen Co., Ltd. (Saitama, Japan) for the use of amateuer astronomers to mount a telescope. We considered here that the equatorial mounting was more reliable than the altazimuth for solar tracking because of its mechanical structure. The equatorial mounting was set at the roof terrace of the Bldg.3 of Engineering, Nagoya University at latitude 35.16 north and longitude 136.96 east, Nagoya, Japan. The polar direction of the equatorial mounting was adjusted in the evening using locations of North Star and some major constellations such as Cassiopeia and Triones.

A continuous lasing experiment of our μSPL was performed on Wednesday, August 9th, 2017. The μSPL experimental rig is pictured in Fig. 4. It was clear weather all day. The weather data were summarized in Table 2. Output power of the μSPL was measured with a power meter sensor (THOLABS S121C) every 0.3 s and the measured value was stored in the memory (THOLABS PM100D), coinstantaneously. A pyrheliometer for the direct solar radiation of 18 mm caliber and a solar telescope were fabricated and mounted on the same equatorial mounting with the μSPL and tracked the sun simultaneously. The power of the direct solar radiation in 5° in view angle and in the wavelength range between 190 nm and 25 μm captured with an aperture and a pinhole was measured with a THOLABS S302C thermal power meter sensor attached to the pyrheliometer. These continuous measurements were recorded in a separate THOLABS PMD100D every 0.3 s. The THOLABS S302C power meter sensor had been calibrated with an EKO INSTRUMENTS MS-53 (ISO 9060 First Class Pyrheliometer) which gave the value of the direct solar radiation in a unit of W/m^2. The insert at the lower left in Fig. 4 is an image of the sun on a personal computer (PC) display monitored by the solar telescope using a video-capturing attachment GV-D4HVR supplied by I-O DATA DEVICE, INC.. As reference, global solar irradiance was measured with YOKOGAWA digital illuminometer 51001. Qualitative measurements of temporal insolation were monitored using an Ocean Optics MAYA2000 solid state optical spectrum analyzer.

After adjustment of the direction of the μSPL roughly using the sun image on the PC display monitored by the solar telescope, precise adjustment of screws fixing the μSPL onto the mounting gave sudden rise of the output power of the μSPL from several μW to several mW at

Table 1
Captions for abbreviations in Fig. 3.

Abbreviation in Fig. 3	Specifications and roles
LM	Custom ordered Nd:1%, Cr:0.1% co-doped YAG ceramic cylindrical laser rod of 1 mm in diameter and 10 mm in length
OAP	Off-axis parabolic Al mirror coated with Al (Edmund Optics, #63-187): Reflectance for sunlight: 95% with its focus on F-side of LM. Diameter of the caliber: 76.2 mm. The sunlight concentration ratio is about 1×10^{-4}
HR	Multilayered thin film optical filter coated on F-side of LM by custom order. Transmittance of sunlight coming from OAP for pumping LM:95% in the wavelength λ between 440 and 850 nm. Reflectance of the emitted light at λ = 1064 nm coming from Nd in LM: 99.95% (to boost laser oscillation)
BBAR	Multilayered thin film optical filter coated on B-side of LM by custom order. Transmittance of sunlight which was not absorbed in LM: > 95% for 780 nm < λ < 1064 nm. Transmittance of the light of λ = 1064 nm emitted from Nd in LM: 100%
OC	Output coupler of curvature radius 100 mm with a dielectric multilayer of a reflectance of 99% at λ = 1064 nm (LCM99-25C05-100-1064 supplied by SIGMAKOKI, Japan) to compose resonator reflecting the laser output back to LM
BPF	Bandpass filter (THOLABS FL1064-10) of T = 70% at the narrow wavelength range λ = 1064 ± 2 nm and FWHM of the transmittance of 10 ± 2 nm to transmit the laser light selectively

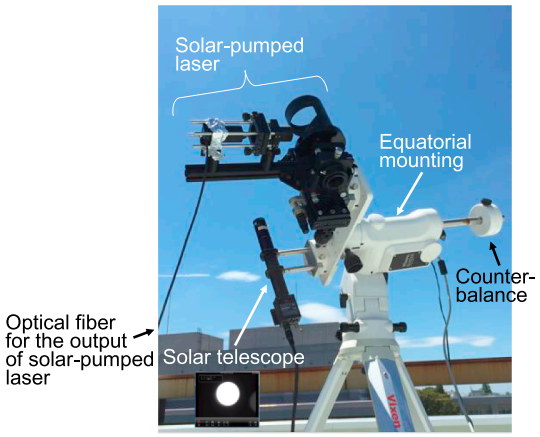

Fig. 4. A solar-pumped laser system tracking the sun automatically on an equatorial mounting (VIXEN SXD2). The insert at the lower left is an image of the sun on a PC display monitored by the solar telescope using a video-capturing attachment for a rough adjustment of direction of μSPL toward the sun.

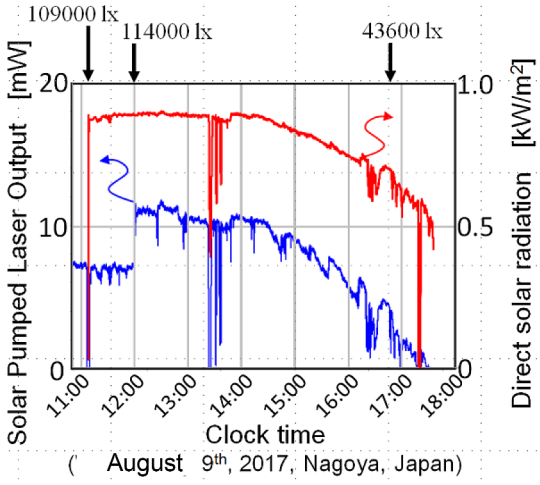

Fig. 5. Variation of the solar-pumped laser output power as a function of time with an occasional manual readjustment of equatorial mount during automatic solar tracking. Variation of the direct solar radiation in the unit of kW/m^2 measured by a pyrheliometer is also shown. The measured global solar irradiance in the unit of lx at three different clock times are shown at the upper side, for reference.

Table 2
The weather data.

	Official weather data
Observation point	Nagoya Local Meteorological Office at 1.4 km north from the experimental site on the same longitude
The high temperature of the day	34.4 °C at 14:46
The low temperature of the day	25.6 °C at 3:21
Atmospheric pressure	990.8 hPa
Steam pressure	23.5 hPa
Average humidity	57%
The lowest humidity	41% at 18:31

10:50, indicating laser oscillation was taking place. After the beginning of the μSPL oscillation, the solar telescope was replaced by the pyrheliometer, and the measurement of the direct solar radiation was performed in parallel with the measurement of the output power of the μSPL.

3. Results

Fig. 5 shows the variation of the μSPL output power as a function of time in the lower blue[1] line. The variation of the direct solar radiation in the unit of kW/m^2 is also shown in the upper red line. The global solar irradiances at three different clock times indicated on the illuminometer: 109,000 lx at 11:08, 114,000 lx at 11:59, and 43,600 lx at 16.48 are also shown at the upper side of the figure, for reference. Synchronism detection between the output power of the μSPL and the direct solar radiation was confirmed by shading the sunlight manually with a black board instantaneously at about 11:07. Simultaneous instantaneous falls both in the μSPL output and in the direct solar radiation around 13:22–13:36 and 17:17 were caused by passing clouds. With occasional manual readjustments of the equatorial mounting such as at 11:10, 11:23, 11:33, 11:43, 11:52, 12:00, 12:25, 12:55, 13:48, 14:46, 15:16, 15:37, 16:11, 16:29, and 17:00, the output power recovered 2–3 mW. Especially the readjustment at 12:00 gave about 4.5 mW increase in the μSPL output. The maximum direct solar

[1] For interpretation of color in Fig. 5, the reader is referred to the web version of this article.

radiation over 898 W/m^2 took place between 12:00 and 13:00 in which the μSPL output also took its maximum around 12 mW. The μSPL output kept going over 10 mW until 14:30. After continuous decrease, the output power of the μSPL suddenly fell from 0.2 mW level to 0.0017 mW level between 17:34 and 17:35, although instantaneous oscillations were observed several times beyond 17:35. After 17:35 until 17:51, almost all the measured output powers were around 0.0017 mW. Therefore it is considered that the μSPL stopped continuous oscillation between 17:34 and 17:35. It was a good news that μSPL kept continuous oscillation even if the direct solar radiation was lower than 550 W/m^2 around 17:30, that is, 61% of the maximum value. This indicates the possibility of continuous oscillation for 11 h from 6:30 to 17:30 which is quite longer than our expectation and favorable for solar-energy utilization.

The datasets corresponding to the μSPL output: 80,562 datasets of (an ordinal number, the time A, μSPL output), and to the direct solar insolation 76,977 datasets (an ordinal number, the time B, the direct solar insolation), were not consistently aligned to an elapsed time after the first sampling at the ordinal number 1. Although both measurements were made in general every 0.3 s, there were occasional misses in saving the data or deviations in the time step length. While these issues did not significantly affect the overall trends in μSPL output vs. clock time, they would cause local inaccuracies in a plot of μSPL output vs. solar insolation. The datasets were therefore processed into a pseudo-synchronous dataset by eliminating the corresponding data point from μSPL when a solar insolation data point was missing and vice versa. Moreover, if the difference between the time A and B exceeded 0.15 s, the dataset was rearranged to form a new dataset having the time differences within 0.14 s.

Fig. 6 shows a plot of these synchronous 47,012 data sets, that is, the plot of the μSPL output against the incident direct sunlight power at the OAP The distribution of the data clearly teaches the existence of a threshold incident direct sunlight power around 2.05 W for laser oscillation and the linear increase of the μSPL output power with the incident direct sunlight power larger than 2.05 W. Since a LM must be optically pumped sufficiently before it makes laser oscillation, existence of the threshold power over which the output power begins to increase with the pumping power is a clear evidence of laser oscillation taking place. This plot was realized because the measurement and the data acquisition of the μSPL output power were continued beyond 17:30 after the oscillation stopped because of shadowing of sunlight power by the cloud spreading flat to the western horizon. Although the fundamental theory of laser (Svelto, 2010; Traeger, 2012; Yariv and Yeh, 2007) teaches the linear increase in the output power of laser with increase in the input pumping power, a more detailed inspection of Fig. 6 reveals existence of two straight lines with approximately the same x-intercept: one is that in the region under 2.7 W of the total incident power (under 5 mW of the μSPL output), and the other is the one in the region over 2.7 W of that (over 5 mW of the μSPL output), with an inflection point around 2.7 W. Since the μSPL output was over 5 mW in the major day time before 16:30 in this experiment as shown in Fig. 5, we estimated the external slope efficiency to be 0.82% from the straight line over 2.7 W. The slope efficiency based on the straight line below 2.7 W is discussed later in this section using the inserted figure in Fig. 6. The external slope efficiency obtained here is the increase in the output power of μSPL divided by the corresponding increase in the incident direct sunlight power to OAP in the region beyond the threshold incident direct sunlight power around 2.05 W. It should be noted that the threshold power here does not stand for the threshold sunlight power absorbed in the LM as usually defined in laser physics (Svelto, 2010; Traeger, 2012; Yariv and Yeh, 2007), but stands for the threshold total incident sunlight power at the entrance of the OAP. In the same sense, the external slope efficiency here stands for the ratio of the increase of the output power of μSPL not to the increase of the absorbed sunlight power in the LM as usually defined in laser physics (Svelto, 2010; Traeger, 2012; Yariv and Yeh, 2007), but to the increase of the total

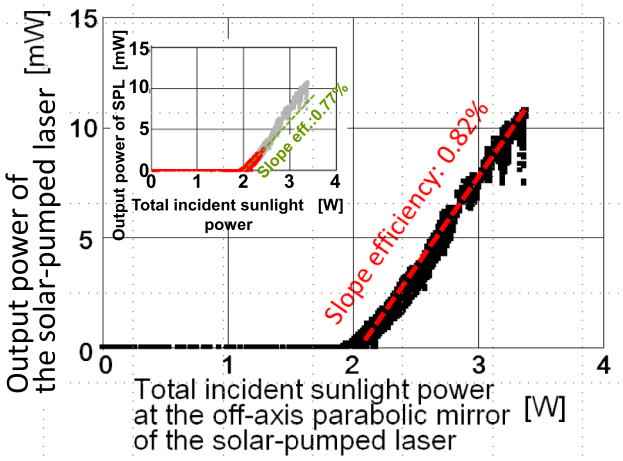

Fig. 6. Plots of the μSPL output power against the incident direct sunlight power at the OAP using the 47,012 data sets from those shown in Fig. 5. The insert at the upper left is a replot emphasizing the 8000 data points which correspond to the last 40 min after 16:50 by red markers while others by gray markers. (For interpretation of the references to color in this figure legend, the reader is referred to the web version of this article.)

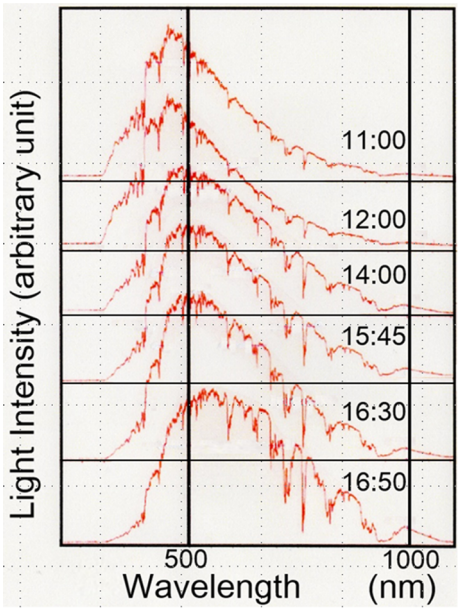

Fig. 7. Variation of the measured solar spectrum as a function of the clock time for reference.

incident sunlight power at the entrance of OAP. Therefore, the threshold power and the slope efficiency in this definition depend not only on the LM but also on the total performance of the SPL system including the performance of the sunlight collection optical system. These definitions are important when the μSPL is considered as a means of solar energy conversion device.

Fig. 7 shows variation of the measured solar spectrum as a function of the clock time. Since the measured intensities overflowed when the optical fiber for solar spectrum sampling was directed at the sun, it was directed manually at a direction near the sun at which the measured intensities did not overflow as a stopgap measure. Therefore, the absolute intensities of the measured spectra did not have any meaning but the shapes of the spectra qualitatively teaches the existence of a gradual red-shift of the peak of the solar spectrum as the afternoon grew late. To know whether this red shift influenced the oscillation properties of the μSPL or not, a replot is shown in the insert at the upper left in Fig. 6 in

which the 8000 data points measured in the last 40 min after 16:50 are indicated by the red markers while the others in the gray markers. Those data of the red markers were measured under the insolation with the spectrum almost equal to or more redshifted than that at 16:50 indicated in Fig. 7. The distribution of the red markers is consistent with the second straight line below 2.7 W of the total incident power described above. The slope efficiency deduced from this second straight line is evidently lower than that deduced from the total data in the main figure. To compare the slope efficiency qualitatively, the external slope efficiency of 0.77% was deduced from the second straight line while that deduced from the first line was 0.82%. The two straight lines do not positively indicate the existences of two different threshold incident direct sunlight powers for laser oscillation but the same one around 2.05 W.

4. Discussion

The present work addresses one of the two blank walls for the development of SPLs for solar energy utilization and was successful in attaining continuous oscillation for more than 6 h and 30 min as shown in Fig. 5 by downsizing the SPLs to "μSPL" so as to reduce the effect of wind load by the rigid mechanical structure and the low stature, and so as to enhance thermal dissipation in the thin LM. Here, the present results are evaluated with the discussion on the threshold power and the slope efficiency obtained from Fig. 6. The value of the abscissa axis in Fig. 6 is the direct sunlight power harvested by the active area of the caliber of OAP. In the present study, the diameter of the caliber is 76.2 mm. Subtracting the thickness of the casing trim of the UV filter, the active diameter is 69.0 mm. Therefore, the active area is 37.4 cm^2. The threshold incident direct sunlight power obtained from Fig. 6 is 2.05 W. Therefore, the threshold incident sunlight power density per area is 54.8 mW/cm^2. The maximum incident direct sunlight in Fig. 6 is 3.36 W. This corresponds to 89.8 mW/cm^2. For reference, 1 Sun at AM1.5g (global) is 100 mW/cm^2, and corresponding AM1.5d (direct) is 90 mW/cm^2 (Gueymard et al., 2002). The maximum incident direct sunlight density in Figs. 5 and 6 was almost the same as that of AM1.5d at 1 Sun. The threshold incident sunlight power density is almost 61% of that. The incident direct sunlight power 2.7 W around which the oscillation property showed an inflection point in Fig. 6, corresponds to the incident sunlight power density of 72.2 mW/cm^2: 80% of the direct incident power density of that of AM1.5d at 1 Sun. The incident direct sunlight density was kept larger than this until 16:30, that is, in almost all the daytime. Therefore, the slope efficiency was 0.82% in almost all the day time. The absolute value of this slope efficiency is much lower than our best value of 1.75% obtained in September 2015 as shown in Fig. 8 using the same laser rod as in the present study. Some mean

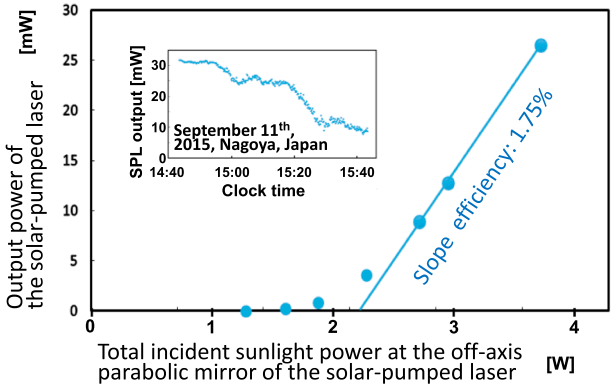

Fig. 8. Plots of the μSPL output power against the incident direct sunlight power at the OAP using partial masking of the sunlight at the entrance of the OAP. The insert at the upper left is a variation of the solar-pumped laser output power in one hour continuous oscillation.

pollution on the surface of OAP, OC and laser rod itself may have caused this decrease in slope efficiency in these 23 months. Some mean miss adjustment may have also caused this. In addition, some deterioration of LM caused by focused sunlight, often called as solarization may have also caused this even if the UV filter was attached in the entrance of the OAP. The threshold value in Fig. 8 was around 2.2 W, a little bit higher than the 2.05 W in Fig. 6. We do not think that this difference is meaningful positively. Fig. 8 was obtained by using partial masking of the sunlight at the entrance of the OAP to change the total incident sunlight power. This is a usual way of the measurement of the oscillation properties of SPL. In contrast, the way how Fig. 6 was obtained is special, and may be the first example obtained from long continuous oscillation experiment until the time late in the afternoon to our knowledge. In the experiment in Fig. 8, preliminary experiment of continuous oscillation for 1 h was also performed using an altazimuth instrument (Vixen SKYPOD) for solar tracking as shown in the insert in Fig. 8 (Motohiro et al., 2017).

Taking all the loss of the optical system including transmittance of the UV filter around 95%, reflectivity of the OAP around 92% and accompanied Fresnel reflection loss into consideration, the actual input power of the direct sunlight in the LM is estimated to be 71.5% of the values on the abscissa axis in Fig. 6 or in Fig. 8. Therefore, the threshold power and the slope efficiency are 1.47 W and 1.15%, respectively in the case of Fig. 6, and 1.57 W and 2.45% in the case of Fig. 8, standing for usual definitions in laser physics (Svelto, 2010; Traeger, 2012; Yariv and Yeh, 2007). As for the present simple homogeneous Nd/Cr:YAG ceramic laser rod, the slope efficiency 2.45% mentioned above, is one of the highest values for single mode oscillation of laser rods (Mehellou et al., 2017).

As for the lower slope efficiency: 0.77% obtained after 16:30 in the region of direct incident sunlight power below 2.7 W, its relation to the red shift of the solar spectrum is discussed below.

We have also studied energy transfer efficiency from Cr^{3+} to Nd^{3+} in Nd (1.0 at.%)/Cr (0.4 at.%) co-doped YAG transparent ceramics medium in the laser oscillation states (Hasegawa et al., 2015). The laser oscillation has performed using two pumping lasers operating at 808 nm and 561 nm; the former pumps Nd^{3+} directly to create the 1064 nm laser oscillation, whereas the latter assists the performance via Cr^{3+} absorption and sequential energy transfer to Nd^{3+}. From the laser output power properties and laser mode analysis, the energy transfer efficiency was determined to be around 65%, which is close to that obtained from the spontaneous Nd^{3+} emission. The red shift may be more favorable for optical absorption around 808 nm by Nd^{3+} ions in the LM, and even for optical absorption around 561 nm by Cr^{3+} ions in the LM. On the other hand, since Cr^{3+} has another broadband absorption between 400 nm and 500 nm, the sunlight in this wavelength range may also have contributed to the 1064 nm laser oscillation. The observed red shift of the solar spectrum may have caused considerable loss of absorption in this wavelength range. Therefore, it is not straightforward to understand the decrease in the slope efficiency in relation to the red shift of the solar spectrum. More detailed inspection should be done in the laboratory based on the observed phenomena and the data in the present outdoor experiment.

The continuous oscillation presented in this paper is reproducible although it depends on the weather of the day. We experienced continuous oscillations (a) from 14:40 to 15:40 as shown in Fig. 8, (b) from 10:41 to 13:23, (c) from 10:56 to 13:31, and (d) from 12:00 to 15:56, on different days. In the case of (c), the continuous oscillation actually restarted from 13:37 to 15:47, showing possibility of a continuous oscillation from 10:56 to 15:47, that is, a continuous oscillation of 4 h and 51 min if there was not a 6 min interval between 13:31 and 13:37.

After the discussion on the continuous oscillation addressed in the present work, our research activities to address the other blank wall for the development of SPLs for solar energy utilization, that is, low sunlight-to-laser energy conversion efficiency are described briefly because both of the two blank walls must be overcome for SPLs to be used as a

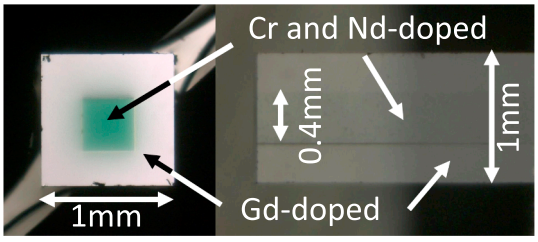

Fig. 9. Photographs of a core (Cr and Nd-doped) and cladding (Gd-doped to match the refractive index with the core) type YAG ceramic laser rod for μSPL.

means of solar-energy utilization. Although theoretical upper limit of the energy conversion efficiency of SPL employing a Nd:YAG LM is around 31% (Nechaev and Rotschild, 2017), most of the efficiencies reported were around 10% (in multimode oscillation, much lower in single mode) or lower. We have been addressing this problems employing a core-cladding type YAG ceramic laser rod (the cladding: Gd-doped YAG, the core: Nd/Cr:YAG) into to the present μSPL to improve the mode-matching efficiency as shown in Fig. 9 (Hasegawa et al., 2018). In this core-cladding type ceramic laser rod, the sunlight is absorbed not in the cladding but only in the core in which the main lasing mode region is involved. The Gd doped in the cladding does not absorb the sunlight, but compensates the difference in the refractive indices between the core and the cladding in the wavelength area where core absorbs the sunlight significantly. Without this compensation, significant amount of the sunlight which is not absorbed in the first pass in the laser rod and goes out of the B-side edge of the laser rod is emitted toward the directions out of the diameter of the OC and is not reflected back into the rod to contribute again for lasing, lowering the conversion efficiency. According to our preliminary calculation, the employment of the core-cladding type ceramic laser rod in our μSPL is to bring the possibility of the efficiency approaching 31%. Since this research on this core-cladding type laser rod is a topic being different from the present continuous laser oscillation, it is to be reported separately. Keeping the style of the simple homogeneous Cr/Nd:YAG ceramic laser rod, we have also observed that increase of Cr content up to 0.7% causes the 4 times increase of μSPL output under the solar-pumping. This is also a topic on improvement of the efficiency of μSPL to be reported separately from the present continuous oscillation study. To improve the spectral matching efficiency, we also think it promising to employ a vertical cavity surface emitting laser (Quarterman and Wilcox, 2015) which is essentially a disk-type LMs shown in the top right corner in Fig. 2 as a future choice, in place of the present Nd:YAG rod-like LM in our μSPL.

5. Conclusion

In summary, the record long continuous laser oscillation of our μSPL for more than 6 h and 30 min from 10:50 to 17:33 was successfully monitored. Clear lasing properties: existences of a threshold input power and a linear increase of the μSPL output power with the incident direct sunlight power at the OAP were also observed. The solar spectrum monitoring tentatively performed concurrently with the laser oscillation suggested the existence of the red shift in the late afternoon which seemed, however, no significant effect on the lasing of the μSPL. This continuous oscillation can be attributed to the compactness of our μSPL which is advantageous for cooling of the LM and the rigidness against the wind load. This is an indispensable experimental step if SPLs are to be applied to terrestrial solar energy utilization together with other two important challenges. One is the sunlight harvesting on the large ground area which obviously contradicts the compactness of the μSPL with a small aperture area, and the other is the increase in the sunlight-to-laser energy conversion efficiency. The former challenge has been also addressed employing arrays of the present μSPLs with a coordinated solar tracking system as has been separately reported, and the latter challenge is addressed employing core-cladding type laser rod for the present μSPL in which the core is made of Cr/Nd:YAG ceramics and the cladding is made of Gd doped YAG cladding which has the same refractive index with the core but does not absorb the sunlight in the wavelength area where core absorbs the sunlight significantly as has been also reported separately.

Funding

This study was partially supported by Advanced Low Carbon Technology Research and Development Program (ALCA), Japan Science and Technology Agency.

Acknowledgments

The authors would like to express their thanks to JSPS Core-to-Core Program (B. Asia-Africa Science Platform) “Establishment of Research Hub for Compact Mobility in the ASEAN Region” for sending an exchange student from Vietnam to help this experiment.

References

Almeida, J., Liang, D., Vistas, C.R., Bouadjemine, R., Guillot, E., 2015. 5.5W continuous-wave TEM_{00}-mode Nd:YAG solar laser by a light-guide/2 V shaped pump cavity. Appl. Phys. B, Laser Opt. 121, 473–482.
Arashi, H., Oka, Y., Sasahara, N., Kaimai, A., Ishigame, M., 1984. A solar-pumped cw 18W Nd:YAG laser. Jpn. J. Appl. Phys. 23, 1051–1053.
Belousova, I.M., Danilov, O.B., Mak, A.A., Belousov, V.P., Zalesslii, V.Y., Grigor'ev, V.A., Kris'ko, A.V., Sosnov, E.N., 2001. Feasibility of the solar-pumped fullerene–oxygen–iodine laser (Sun-Light FOIL). Opt. Spectrosc. 90, 773–777.
Dinh, T.H., Ohkubo, T., Yabe, T., 2014. Development of solar concentrators for high-power solar-pumped lasers. Appl. Opt. 53, 2711–2719.
Endo, M., 2007. Feasibility study of a conical-toroidal mirror resonator for solar-pumped thin-disk lasers. Opt. Express 15, 5482–5493.
Gueymard, C., Myers, D., Emery, K., 2002. Proposed reference irradiance spectra for solar energy systems testing. Sol. Energy 73, 443–467.
Hasegawa, K., Ichikawa, T., Takeda, Y., Ikesue, A., Ito, H., Motohiro, T., 2018. Lasing characteristics of refractive index-matched composite YAG rods employing transparent ceramics for solar-pumped lasers. Jpn. J. Appl. Phys. 57 042701(5 pages).
Hasegawa, K., Ichikawa, T., Mizuno, S., Takeda, Y., Ikesue, A., Ito, H., Ikesue, A., Motohiro, T., Yamaga, M., 2015. Energy transfer efficiency from Cr^{3+} to Nd^{3+} in solar-pumped laser using transparent Nd/Cr:$Y_3Al_5O_{12}$ ceramics. Opt. Express 23, A519–A524.
Ide, T., 2017. (National Institute of Advanced Industrial Science and Technology: AIST), private communications in 2017.
Ikesue, A., Aung, Y.L., 2008. Ceramic laser materials. Nat. Photon. 2, 721–727.
Ikesue, A., Aung, Y.L., Lupei, V., 2013. Ceramic Lasers. Cambridge University Press, New York, pp. 121.
Ito, H., Hasegawa, K., Mizuno, S., Motohiro, T., 2012. A solar-pumped micro-rod laser without active cooling. In: Proceedings of the 1st Advanced Lasers and Photon Sources Conference ALPS'12, (Laser Society of Japan), pp. 2 (paper ALPS12 2p-20).
Kiss, Z.J., Lewis, H.R., Duncan, R.C., 1963. Sun pumped continuous optical maser. Appl. Phys. Lett. 2, 93–94.
Lee, J.H., Weaver, W.R., 1981. A solar simulator-pumped atomic iodine laser. Appl. Phys. Lett. 39, 137–139.
Liang, D., Almeida, J., Vistas, C.R., Guillot, E., 2017. Solar-pumped Nd:YAG laser with 31.5 W/m^2 multimode and 7.9 W/m^2 TEM_{00}-mode collection efficiencies. Sol. Energy Mater. Sol. Cells 159, 435–439.
Maiman, T.H., 1960. Stimulated optical radiation in ruby. Nature 187, 493–494.
Masuda, T., Iyoda, M., Yasumatsu, Y., Endo, M., 2017. Low-concentrated solar-pumped laser via transverse excitation fiber-laser geometry. Opt. Lett. 42, 3427–3430.
Mehellou, S., Liang, D., Almeida, J., Bouadjemine, R., Vistas, C.R., Guillot, E., Rehouma, F., 2017. Stable solar-pumped TEM_{00}-mode 1064 nm laser emission by a monolithic fused silica twisted light guide. Sol. Energy 155, 1059–1071.
Mizuno, S., Ito, H., Hasegawa, K., Suzuki, T., Ohishi, Y., 2012. Laser emission from a solar-pumped fiber. Opt. Express 20, 5891–5895.
Mizuno, S., Hasegawa, K., Ichikawa, T., Ito, H., Motohiro, T., Suzuki, T., Ohishi, Y., 2014. Solar-pumped lasers for photovoltaic energy conversion. In: Tech. Dig. of the 6th World Conf. Photovoltaic Energy Conversion, pp. 29–30.
Mori, M., Nagayama, H., Saito, Y., Matsumoto, H., 2004. Summary of studies on space solar power systems of the National Space Development Agency of Japan. Acta Astronaut. 54, 337–345.
Motohiro, T., Ichiki, A., Ichikawa, T., Ito, H., Hasegawa, K., Mizuno, S., Ito, T., Kajino, T., Takeda, Y., Higuchi, K., 2015. Consideration of coordinated solar tracking of an array of compact solar-pumped lasers combined with photovoltaic cells for electricity generation. Jpn. J. Appl. Phys. 54, 08KE04.
Motohiro, T., Takeda, Y., Ito, H., Hasegawa, K., Ikesue, A., Ichikawa, T., Higuchi, K., Ichiki, A., Mizuno, S., Ito, T., Yamada, N., Luitel, H.N., Kajino, T., Terazawa, H.,

Takimoto, S., Watanabe, K., 2017. Concept of the solar-pumped laser-photovoltaics combined system and its application to laser beam power feeding to electric vehicles. Jpn. J. Appl. Phys. 56, 08MA07.
Nechaev, S., Rotschild, C., 2017. Detailed balance limit of efficiency of broadband-pumped lasers. Sci. Rep. 7 11497(1–6).
Ohkubo, T., Yabe, T., Yoshida, K., Uchida, S., Funatsu, T., Bagheri, B., Oishi, T., Daito, K., Ishioka, M., Nakayama, Y., Yasunaga, N., Kido, K., Saito, Y., Baasandash, C., Kato, K., Yanagitani, T., Okamoto, Y., 2009. Solar-pumped 80 W laser irradiated by a Fresnel lens. Opt. Lett. 34, 175–177.
Payziyev, S., Makhmudov, K., 2016. Solar pumped Nd:YAG laser efficiency enhancement using Cr:LiCAF frequency down-shifter. Opt. Commun. 380, 57–60.
Pe'er, I., Vishnevitsky, I., Naftali, N., Yogev, A., 2001. Broadband laser amplifier based on gas-phase dimer molecules pumped by the Sun. Opt. Lett. 26, 1332–1334.
Quarterman, A.H., Wilcox, K.G., 2015. Design of a solar-pumped semiconductor laser. Optica 2, 56–61.
Simpson, G.R., 1964. Continuous sun-pumped room temperature glass laser operation. Appl. Opt. 3, 783–784.
Saiki, T., Motokoshi, S., Imasaki, K., Fujioka, K., Fujita, H., Nakatsuka, M., Izawa, Y., Yamanaka, C., 2008. Effective fluorescence lifetime and stimulated emission cross-section of Nd/Cr:YAG ceramics under CW lamplight pumping. Jpn. J. Appl. Phys. 47, 7896–7902.
Saiki, T., Taniguchi, S., Nakamura, K., Iida, Y., 2017. Development of solar-pumped lasers and its applications. Electr. Eng. Japan 199, 3–9.
Suzuki, T., Kawai, H., Nasu, H., Hughes, M., Ohishi, Y., Mizuno, S., Ito, H., Hasegawa, K., 2011. Quantum efficiency of Nd^{3+}-doped glasses under sunlight excitation. Opt. Mater. 33, 1952–1957.
Svelto, O., 2010. Principles of Lasers. Springer, New York, pp. 263.
Terry, C.K., Peterson, J.E., Goswami, D.Y., 1996. Terrestrial solar-pumped iodine gas laser with minimum threshold concentration requirements. J. Thermophys. Heat Transfer 10, 54–59.
Traeger, F. (Ed.), 2012. Springer Handbook of Lasers and Optics. Springer, Berlin, pp. 660.
Yariv, A., Yeh, P., 2007. Photonics. Oxford University Press, New York, pp. 246.
Young, C.G., 1966. A sun-pumped cw one-watt laser. Appl. Opt. 5, 993–997.